The Linnean Society of London BIOLOGICAL Journal of the Linnean Society

Biological Journal of the Linnean Society, 2016, **117**, 463–481. With 3 figures.

Ecomorphological diversification following continental colonization in muroid rodents (Rodentia: Muroidea)

BADER H. ALHAJERI[1,2]*, JOHN J. SCHENK[1,3] and SCOTT J. STEPPAN[1]

[1]*Department of Biological Science, Florida State University, Tallahassee, FL, 32306-4295, USA*
[2]*Department of Biological Sciences, Kuwait University, Safat, 13110, Kuwait*
[3]*Department of Ecology and Evolutionary Biology, Tulane University, New Orleans, LA, 70118-5698, USA*

Received 7 July 2015; revised 28 August 2015; accepted for publication 28 August 2015

The emergence of exceptionally diverse clades is often attributed to ecological opportunity. For example, the exceptional diversity in the most diverse superfamily of mammals, muroid rodents, has been explained in terms of multiple independent adaptive radiations. If multiple ecological opportunity events are responsible for generating muroid diversity, we expect to find evidence of these lineages ecologically diversifying following dispersal into new biogeographical areas. In the present study, we tested the trait-based predictions of ecological opportunity using data on body size, appendages, and elevation in combination with previously published data on biogeographical transitions and a time-calibrated molecular phylogeny. We identified weak to no support of early ecological diversification following the initial colonizations of all continental regions, based on multiple tests, including node height tests, disparity through time plots, evolutionary model comparison, and Bayesian analysis of macroevolutionary mixtures. Clades identified with increased diversification rates, not associated with geographical transitions, also did not show patterns of phenotypic divergence predicted by ecological opportunity, which suggests that phylogenetic diversity and phenotypic disparity may be decoupled in muroids. These results indicate that shifts in diversification rates and biogeographically-mediated ecological opportunity are poor predictors of phenotypic diversity patterns in muroids. © 2015 The Linnean Society of London, *Biological Journal of the Linnean Society*, 2016, **117**, 463–481.

ADDITIONAL KEYWORDS: appendage morphology – biogeography – body mass – disparity – diversity – ecological opportunity – elevation – evolutionary rate – phenotype – South America.

INTRODUCTION

The generality of adaptive radiation in evolutionary diversification has often been investigated recently using the ecological opportunities (EO) model (Harmon *et al.*, 2003, 2008a, b, 2010; Rabosky & Lovette, 2008). Causes of EO include biogeographical transitions, mass extinctions of competitors, and/or the evolution of key innovations, which allow lineages to exploit new and underutilized adaptive zones and lead to rapid adaptive divergence (Simpson, 1953; Schluter, 2000a; Grant & Grant, 2008; Yoder *et al.*, 2010). Two main predictions of EO are: (1) an early increase in the rate of phylogenetic and phenotypic diversification (indicating that lineages are taking advantage of relatively empty niche space as a consequence of underutilized adaptive zones) (Simpson, 1953; Futuyma, 1986; Schluter, 2000a; McCormack & Smith, 2008) and (2) a subsequent more gradual (often density-dependent, Rabosky & Lovette, 2008) decline in the rate of phylogenetic and phenotypic diversification as a result of increased competition as the finite number of niches are filled (Walker & Valentine, 1984; Baldwin & Sanderson, 1998; Schluter, 2000a; Lovette, Bermingham & Ricklefs, 2002; Harmon *et al.*, 2003, 2008a, b, 2010; Yoder *et al.*, 2010). The attendant decline in rates should occur unless some subset of lineages break out into new adaptive zones (creating their own EO, Schluter, 2000a) or rising extinction rates erases previous diversity. Studies have found many cases of early bursts of net diversification that are usually followed by a density-dependent decline in diversification rate (Harmon *et al.*, 2003; Rüber, Zardoya & Ortí, 2005; Kozak, Weisrock & Larson, 2006; McKenna & Farrell, 2006; McPeek, 2008; Phillimore & Price, 2008).

*Corresponding author. E-mail: bader.alhajeri@ku.edu.kw

Tests of the phenotypic predictions of EO have lagged and, among those studies, only a few cases match the expectations (Lovette & Bermingham, 1999; Kozak *et al.*, 2006; Rowe *et al.*, 2011).

Most studies of EO have been conducted in clades of relatively low diversity and narrow geographical distributions (e.g. sticklebacks in British Columbia: Nosil & Reimchen, 2005; North American wood warblers: Rabosky & Lovette, 2008; Galápagos land snails: Parent & Crespi, 2009; Caribbean *Anolis* lizards: Mahler *et al.*, 2010; Mahler *et al.*, 2013). Analyses conducted on small clades, however, might not have sufficient statistical power to detect signatures of EO. Many of these studies are also conducted in island systems, in part because they are smaller and more tractable than the continental or marine radiations that account for most biodiversity. However, recent studies have begun exploring these patterns in larger clades and/or geographical scales (e.g. South American ovenbirds: Derryberry *et al.*, 2011; damselfishes: Frédérich *et al.*, 2013; New World lupines: Drummond *et al.*, 2012; cosmopolitan muroid rodents: Schenk, Rowe & Steppan, 2013; Himalayan birds: Price *et al.*, 2014; bicontinental primate radiation: Tran, 2014).

Muroid rodents, in particular, are optimally suited as a model system to explore EO. They are the most diverse superfamily of mammals, with over 1600 species, representing more than 28% of mammal species diversity (Musser & Carleton, 2005). The exceptional diversity of muroids has been attributed to multiple independent bursts of diversification (Steppan, Adkins & Anderson, 2004) and recent analyses that used molecular phylogenies found widely varying diversification rates among subclades (Fabre *et al.*, 2012; Schenk *et al.*, 2013). Muroids originated in Eurasia and sequentially expanded into most terrestrial habitats on every continent and major landmass except Antarctica and New Zealand (Flynn, Jacobs & Lindsay, 1985; Jansa & Weksler, 2004; Steppan *et al.*, 2004; Fabre *et al.*, 2012; Schenk *et al.*, 2013). Thus, the muroid radiation provides numerous EO experiments, as well as the statistical power afforded by replicated evolutionary events (technically pseudo replicates; multiple independent colonizations of continental regions), to answer the question: what happens to diversity when lineages experience vast new ecological opportunities by colonizing new continental regions?

The present study directly follows from Schenk *et al.* (2013), who studied the effect of biogeographical transitions among continental and biogeographical realms on the diversification process of muroids. They identified 28 continental colonization events, categorizing six of them as primary (defined by the absence of muroids or close relatives in the colonized region; three of these were 'virgin', meaning that no small rodents were present at all) and 22 as secondary (muroids present from previous colonizations). EO did not explain the uneven diversity patterns in muroid clades well; only one (South American colonization) out of the six primary continental colonizations and none of the secondary colonizations fit all the phylogenetic predictions of the EO model (significant burst in early phylogenetic diversification rate followed by a significant decline in that rate). These analyses, however, surveyed phylogenetic patterns only and did not investigate patterns of ecologically important morphological traits that might provide evidence for EO regarding the phenotypic predictions of the model. Schenk *et al.* (2013) also detected increased diversification rates in lineages not associated with biogeographical transitions, which were suggested to be driven by other mechanisms (e.g. mass extinctions of competitors or key innovations) that they had not tested.

Although extinction may erase diversification patterns by pruning lineages, and thus erase the signature of an early burst in diversification (Quental & Marshall, 2009; Harmon *et al.*, 2010), it will not decrease expected disparity (mean or variance) provided that it is random with respect to phenotype (Foote, 1993, 1997; Slater *et al.*, 2010). Similarly, estimates of morphological variance should be unbiased by sampling (Foote, 1997), in contrast to estimates of species diversity. Therefore, evidence for EO may still be detected as a pattern of exceptional phenotypic divergence and evolutionary rate (Harmon *et al.*, 2003; Slater *et al.*, 2010; Martin & Wainwright, 2011), even when exceptional species diversity is not estimated.

In the present study, we use the biogeographical analysis and the diversification framework of Schenk *et al.* (2013) to test the phenotypic predictions of the geographically-mediated EO model: following primary continental colonizations, there will be an early burst in phenotypic evolution and disparity followed by a gradual decline (Simpson, 1953; Schluter, 2000a). We also test the two aforementioned phenotypic prediction of the EO model in lineages that Schenk *et al.* (2013) found to have high diversification rates (regardless of biogeographical transition); these lineages may be experiencing EO driven by other non-biogeographical factors (e.g. key innovations or mass extinctions of competitors).

Predictions of EO are primarily expected to apply to traits that are correlated with niches (Schluter, 2000b) and therefore we test the trait-based predictions of EO in a suite of traits with strong association with niche. Body mass is arguably the single-most ecologically important trait because it is an important predictor of diet (Schluter, 2000b; Kozak *et al.*, 2005; Clabaut *et al.*, 2007) and many aspects of an animal's interactions with the environment (LaBarbera, 1989; Brown, 1995). Relative tail length is strongly

correlated with locomotion and lifestyle, with very short tails in burrowers (where tails have little utility), and with long tails in arboreal species (useful for balance; Lemen, 1980; Fooden & Albrecht, 1999) and cursorial species (counter-balance to high-amplitude hopping; Alexander & Vernon, 1975; Mares, 2009). Appendage morphology is based on a multivariate ordination of body, tail, hindfoot, and ear lengths, which is used to extract a set of variables [principal component (PC) axes] that maximize morphological variance among species, and complement analyses of individual traits (body mass, relative tail length, and elevation). Although these PC axes were not used as a direct ecological index as in the univariate traits, they may reflect habitat use and overall ecology. For example, relative hindfoot length (ratio of hindfoot length to head–body length), similar to relative tail length (ratio of tail length to head–body length), is correlated with gait, particularly with bipedal locomotors in desert environments having an enlarged hindfoot (Berman, 1985). The length of all extremities, including ear length, is expected to vary in accordance with Allen's rule, whereby they tend to increase with increasing temperatures (Allen, 1877). Finally, elevational preference is a major ecological axis on which sister species diverge in various taxa (Endler, 1982; Porter *et al.*, 2002; Navas, 2002; Hall, 2005; Altshuler & Dudley, 2006; Cadena, 2007) and is an important environmental determinant of habitat.

The major objective of the present study is to test the two main phenotypic predictions of the geographically-mediated EO model: following the colonization of a region, there would be a burst of divergence relative to background rates, followed by a decline in those rates. We test our major objective in all lineages that Schenk *et al.* (2013) found to correspond with primary continental colonizations. A minor objective of the present study is to test whether clades that are associated with increased rates of phylogenetic diversification (regardless of biogeographical transitions) also experience the aforementioned two main patterns expected by the EO model, which may provide support for non-geographically-mediated triggers of EO in those clades, such as key innovations or mass extinctions of competitors. Moreover, the second set of analyses serves as a preliminary test of the association between phylogenetic diversification and phenotypic diversification in muroids.

MATERIAL AND METHODS

Phylogenetic diversification and biogeographical framework

We used the chronogram from Schenk *et al.* (2013) that includes 297 muroid species sampled proportional to the total diversity of the clades. This chronogram was estimated using four nuclear genes (BRCA1, GHR, IRBP, and RAG1) totalling 6720 bp, and used 13 fossil calibrations. We used the 28 biogeographical transitions identified by Schenk *et al.* (2013) to determine whether trait-based predictions of EO correspond with colonization of major biogeographical regions (Fig. 1, see also Supporting information, Fig. S1). We focused on primary colonizations because of the possible incumbency effect limiting secondary radiations, and also because no secondary radiations matched phylogenetic predictions of EO. In clades descended from primary colonizations, we pruned species that subsequently dispersed out of the biogeographical region prior to phenotypic diversification analyses. For primary colonizations, we only attributed to them the direct descendants and their autochthonous radiations, treating later colonizations as secondary radiations (in particular, the modern biotas of Africa and Eurasia, which are built from multiple colonizations). This means that, in clades descended from each colonization, we pruned species that subsequently dispersed out of the biogeographical region prior to phenotypic diversification analyses.

Crown muroids originated in Eurasia (Schenk *et al.*, 2013) and their direct descendants accumulated 31 species that remained in Eurasia (of which 10 were sampled). The earliest biogeographical transition was to Africa at 34.1 Mya and this lineage accumulated a species richness of approximately 76 species (24 sampled). North America was then colonized around 27.4 Mya, which led to the accumulation of 156 species (35 sampled). Muroids colonized Madagascar approximately 24.5 Mya, and accumulated 27 species (10 sampled). South-east Asia appears to have been first colonized approximately 21.4 Mya, which led to the accumulation of 194 species (of which 39 were sampled). Muroids colonized South America next, approximately 12.3 Mya, and accumulated 335 species in that region (70 sampled). The last region to be colonized by muroids was Sahul, approximately 9.4 Mya, which led to the local accumulation of 143 species (28 sampled).

Independent of the nodes associated with geographical transitions (a priori identified EO events), Schenk *et al.* (2013) detected over 20 shifts in diversification rates for clades not associated with geographical transitions. Schenk *et al.* (2013) used three methods to detect shifts in diversification rates: Δ_2 parameters (Chan & Moore, 2002, 2005), relative cladogenesis tests (Purvis, Nee & Harvey, 1995; Harmon *et al.*, 2008b), and the stepwise Akaike information criterion (AIC) model selection approach in MEDUSA (Alfaro *et al.*, 2009), and not all nodes were detected by all methods. We analyzed the

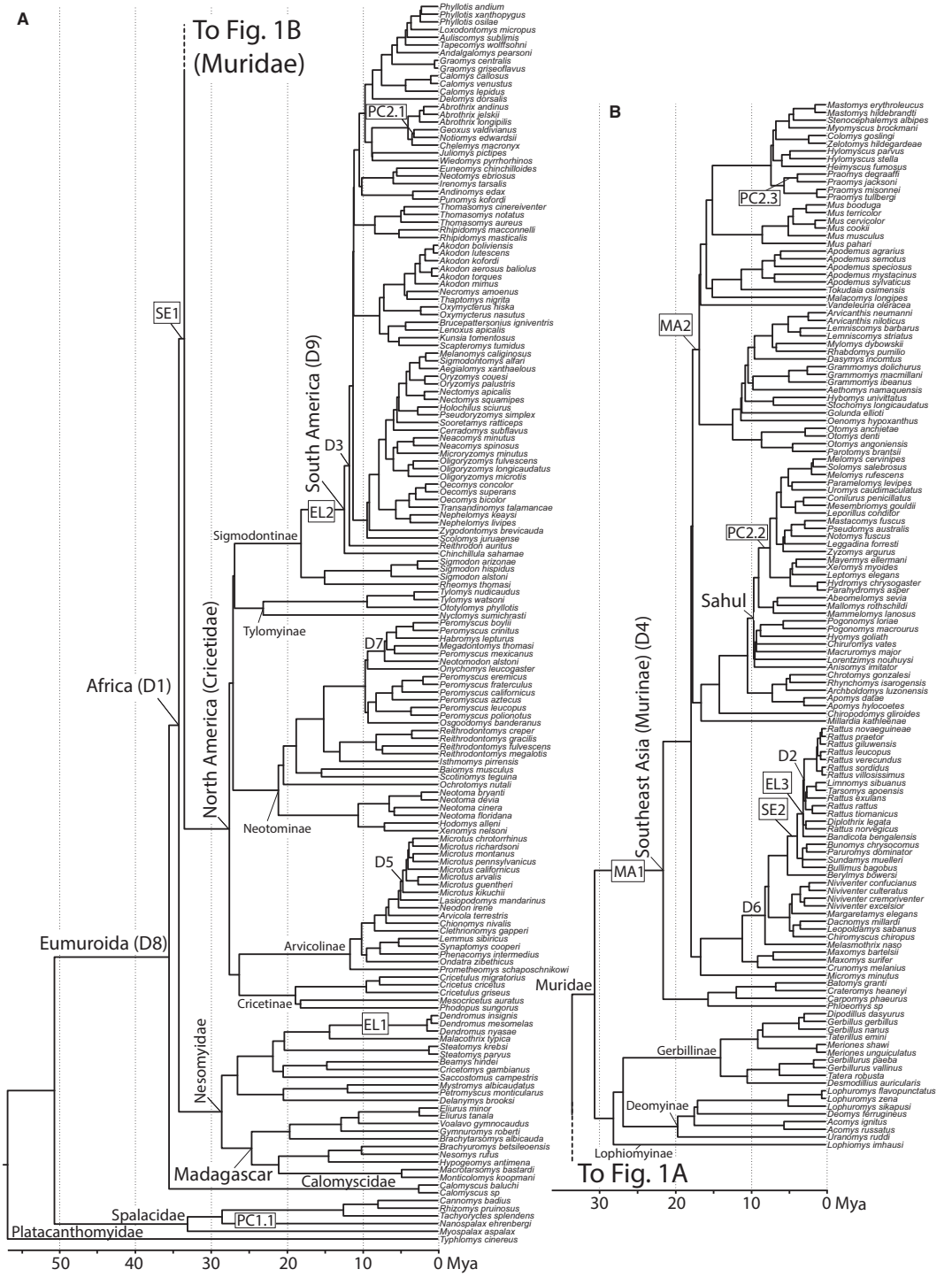

Figure 1. Muroid rodent chronogram modified from Schenk *et al.* (2013). Significant increases in phylogenetic diversification (D1–D9) and primary continental colonizations (see Supporting information, Fig. S1) (both as detected by Schenk *et al.*, 2013) are indicated (Sahul = supercontinent of Australia and New Guinea), along with major taxonomic groups. The rectangles indicate the branches where there was a maximum a posteriori (MAP) rate increase (BAMM analysis) based on the analysis of: SE1-2, speciation–extinction rates; EL1-3, elevation evolutionary rates; MA1-2, mass evolutionary rates; PC1.1, principal component (PC)1 of appendage morphology evolutionary rates; PC2.1-3, PC2 of appendage morphology evolutionary rates. Note: BAMM did not detect any rate slowdowns and the MAP tree for relative tail length indicates no rate shifts. The tree in Fig. 1B is the continuation of the tree in Fig. 1A.

radiations descending from nine nodes: all four nodes that were identified by two or more methods, as well as five additional nodes that received the highest AIC scores in MEDUSA (Fig. 1; diversification nodes 1–9).

Data collection

We compiled data for adults of each species from the literature (both primary sources and summary publications; Nowak, 1999) for body mass (g), as well as head–body length, tail length, hind foot length, and ear length (all mm), and also elevation (m asl) (see Supporting information, Table S1). Mean trait and elevation values were calculated using multiple literature sources when available to minimize the effects of outliers and misreported data (see Supporting information, Table S1). Sexual dimorphism is uncommon in muroids; however, when possible, data were averaged from equal numbers of males and females. Body mass, head–body length, and hind foot length were normalized with log transformations; ear length and tail length were also log-transformed, although only after a value of 0.1 mm was added to all species to account for *Nannospalax ehrenbergi* having no visible ear or tail (=0 mm). Elevation data (mean of the minimum and maximum elevations) were gathered from Musser & Carleton (2005) and GPS coordinates of vouchered specimens from Arctos (2011) using GOOGLE EARTH, version 6.0 (Google, 2010). We conduct phenotypic evolution analyses (see below) on log-transformed body mass, relative tail length (raw tail length divided by raw head–body length), as well as raw elevation.

As a complement to the analyses of the aforementioned three individual traits for which we have strong a priori expectations of ecological association (body mass, relative tail length, and elevation), a more exploratory index of appendage morphology (based on head–body, tail, hind foot, and ear lengths) was estimated using phylogenetic principal component analysis (PPCA) (Revell, 2009) after phylogenetic size correction (Revell, 2009) following the code published in Revell (2009) using the APE library (Paradis, Claude & Strimmer, 2004) in R (R Development Core Team, 2012). Phylogenetic size correction was performed using log body mass. PPCA reduces type 1 error rate by accounting for phylogenetic relationships, making it more conservative than traditional PC analysis in comparative analyses (Revell, 2009). Although Uyeda, Caetano & Pennell (2015) have recently raised concern regarding the use of PC analysis (including PPCA) in comparative analyses, most existing trait evolution methods are univariate, and therefore we analyzed the individual components but interpreted our results from the PC analyses with caution.

Because the choice of size correction has the potential to affect the resulting residual values (Jungers, Falsetti & Wall, 1995), we compared the residuals obtained by phylogenetic size correction with the residuals obtained from two common (nonphylogenetic) size correction methods. The first method calculated the residuals from a linear regression of each variable against body mass. The second method was 'shearing', a method that calculates the residuals from a least squares regression analyses of each trait against the first PC of the pooled data, with the latter used as a size measure (McCoy *et al.*, 2006). Residuals obtained from phylogenetic size correction were highly correlated to residuals obtained from the two nonphylogenetic methods for all four traits (all $R^2_{adj} > 0.90$; $P < 0.000001$; see Supporting information, Table S2). Moreover, we repeated several of our analyses using nonphylogenetic size corrected residuals and we obtained highly similar results (we provide one example in the Supporting information, Fig. S2). Because our choice of size correction method did not appear to significantly affect the results, we used only the phylogenetic size-corrected variables in all subsequent analyses.

PPCA was conducted on a dataset that included log-transformed head–body length, log-transformed tail length, log-transformed hind foot length, and log-transformed ear length. The first and second phylogenetic PC axes described the trait combinations exhibiting the maximum amounts of evolutionary variance in correlated trait evolution, and may detect the consequences of selective divergence that individual traits, accounting for less variance, do not. The first axis was strongly correlated with all measurements except for body length and can be considered as relative extremity size; the second axis was most strongly correlated with ear length and moderately correlated, inversely, with tail length (Table 1). We

Table 1. Loadings of the principal component analysis on appendage morphology

Variable	PC1	PC2	PC3	PC4
Body length	−0.2735	−0.0548	0.8828	0.3780
Tail length	−0.9219	−0.3545	−0.1411	0.0674
Hindfoot length	−0.5499	−0.1918	0.5071	−0.6354
Ear length	−0.5618	0.8271	−0.0184	−0.0026
Eigenvalues	0.0026	0.0014	0.0006	0.0003
% Explained variance	52	29	13	6

Phylogenetic principal component (PC) analysis eigenvalues indicate residual morphology after removal of phylogenetic covariance and do not correspond with ordinary PC analysis eigenvalues (Polly *et al.*, 2013).

also conducted phenotypic evolution analyses (see below) on the PC scores of the first two axes, which together accounted for 81% of the total variance (Table 1) and served as multivariate indices of appendage morphology.

Shift in evolutionary rates

We tested the EO prediction of a significant increase in the rate of phenotypic evolution (Schluter, 2000a) using the censored rate test (CRT) under Brownian motion as implemented in Brownie v2.1 (O'Meara *et al.*, 2006). The CRT compares the fit of two nested models of evolution: a one-rate model for the whole tree and a two-rate model, with separate foreground and background rates, where foreground rates are applied to radiations following continental colonizations. The two models were optimized separately with ML (O'Meara *et al.*, 2006) and the fit of the models was assessed with the AIC (Akaike, 1974). We favoured models that had an AIC score of four or greater (Burnham & Anderson, 2002) after applying a more conservative correction for finite sample sizes (AICc) (Hurvich & Tsai, 1989). The prediction from EO was that evolutionary rate would be significantly greater in the foreground radiation. We use the more general term 'radiation' rather than clade, because for the a priori geographically defined focal groups, most are paraphyletic as a result of the exclusion of emigrant lineages.

Disparity through time

We tested the EO prediction of an early burst in trait divergence, leading to proportionately greater disparity than expected under random models early in radiation history, and a lower proportion of total disparity portioned within recent subclades with disparity through time (DTT) plots in the Geiger library (Harmon *et al.*, 2008a) in R. DTT plots, as implemented in Geiger, plot relative subclade disparity (Harmon *et al.*, 2003). This equals the mean squared pairwise Euclidean distances between all species in morphospace in each subclade whose ancestral lineages were present at that time, relative to the disparity of the entire taxon (Harmon *et al.*, 2003). The DTT plots were used to estimate the morphological disparity index (MDI) (Harmon *et al.*, 2003). We ran 1000 simulations of trait evolution under Brownian motion and compared their mean with the observed plots to calculate the MDI scores (Harmon *et al.*, 2003, 2008b). Because EO predicts disproportionately greater early disparity, we calculated MDI score only of the first third of the DTT plot as a conservative cut-off. A negative MDI score would indicate that early subclade disparity was lower (and among subclade disparity higher) than expected under Brownian motion, which is a result consistent with the EO model (Harmon *et al.*, 2003). Significance was assessed by computing the MDI between each of the 1000 simulated datasets and the observed dataset and then counting the proportion of cases where the MDI score is positive ($\alpha = 0.05$). Because the DTT code in Geiger enabled the analysis of multivariate data, we conducted a multivariate analysis on a matrix that includes log-transformed head–body length, log-transformed tail length, log-transformed hind foot length, and log-transformed ear length and compare the results with those obtained from the univariate PPCA.

Evolutionary rates through time

We tested the EO prediction of a decline in the rate of phenotypic evolution through time (Schluter, 2000a) using the node height test (NHT) (Freckleton & Harvey, 2006), and by testing the fit of the Early Burst (EB) model (Harmon *et al.*, 2010) as implemented in the APE and Geiger libraries in R, respectively. The NHT tests for a relationship between the absolute values of standardized independent contrasts (IC) (Felsenstein, 1985) of the traits with the age of the node that they subtend. In our NHT, we correlated node age (instead of node height) with the standardized independent contrasts because APE uses node age in the calculations; thus, our predictions about the sign of the relationship were the opposite of that from the standard NHT. Because ICs are Brownian rate parameters for the branches over which they are calculated, a significant positive relationship between node age and absolute contrast value indicates that rates of evolution have slowed down through time (Garland, 1992; McPeek, 1995), as would be expected by species subdividing and filling niche space more finely through time (Freckleton & Harvey, 2006).

The EB model of evolution is a random walk model where the rate of evolution decreases exponentially through time. Because the EB model fits traits best that diversify rapidly early in a lineage and then slow down towards the present, it is often used as evidence of the niche-filling model of evolution (Harmon *et al.*, 2010). We assessed the fit of the EB model of evolution by comparing its fit to the data relative to Brownian motion (BM) and Ornstein–Uhlenbeck (OU; which assumes that trait values are attracted to an optimal value) models using AIC (including ΔAIC and AIC weights) models, preferring models with the lowest AIC score, $\Delta AIC = 0$, and with an AIC weight (AICw) closest to 1.

A posteriori detection of rate shifts

In additional to the standard trait-based tests of EO employed above, we also tested the EO hypothesis using Bayesian analysis of macroevolutionary mixtures (BAMM), which quantifies heterogeneity in evolutionary rates across a phylogeny to model complex dynamics of speciation, extinction, and trait evolution (Rabosky, 2014). BAMM uses reversible jump Markov chain Monte Carlo (rjMCMC) to explore candidate models of diversification and trait evolution to find the locations for shifts in evolutionary dynamics that are maximally supported by the data (Rabosky, 2014). Unlike the methods described above, BAMM does not use a priori specifications as to where these shifts in dynamics might have occurred.

We ran a BAMM (version 2.2) speciation–extinction calculation by specifying clade specific sampling fractions (i.e. sampling probabilities) to analytically account for nonrandom and incomplete taxon sampling within muroid clades (Rabosky, 2014). To estimate sampling frequencies, clades were split into tribes if they are well defined based on recent literature (e.g. Musser & Carleton, 2005; Lecompte *et al.*, 2008. In clades where tribal designations were not well defined, we specified sampling fractions at the subfamily level. *Calomyscus* represented the monogeneric family Calomyscidae and *Typhlomys* represented the family Platacanthomyidae (containing two small genera). Sampling frequencies for each clade are listed in the Supporting information (Table S3). We used Musser & Carleton (2005) with updated species numbers from more recent sources (e.g. the tribal classification of Chevret & Dobigny, 2005 to specify Gerbillinae tribes).

We used the Bammtools library (Rabosky *et al.*, 2014) in R to estimate a set of starting parameters for the priors on rate parameters that are consistent across different scaling of the phylogeny. The rjMCMC chain was run for 10^7 generations, sampling every 2000 steps, to give a total of 5000 samples from the posterior; all other parameters were set to the default values. Convergence of the rjMCMC chain was checked using the Coda library (Plummer *et al.*, 2010) in R and Bammtools was used to run post-BAMM analyses and visualizations.

We also ran the a BAMM trait evolution analyses for each of the five ecomorphological traits described above using the same parameters described for the speciation–extinction calculations. As in other analyses, species missing ecomorphological data were pruned from the tree prior to the BAMM analysis.

For the speciation–extinction and each of the trait evolution analyses, we extracted both the maximum a posteriori (MAP) probability tree that detects the single rate shift configuration with the highest posterior probability, and the maximum shift credibility (MSC) tree that estimates the shift configuration that maximizes the marginal probability of rate shifts along branches (Rabosky, 2014). The BAMM results using the MAP criterion matched closely the results based on the MSC criterion. For this reason, and because Rabosky (2014) recommends using MAP for most trees, except trees with thousands of taxa (where MSC is more useful), we discuss only the BAMM results based the MAP criterion. We also extracted rates of diversification and trait evolution through time using the time-variable model in BAMM to determine whether there was an overall slow-down or speed-up in rates over time in Muroidea.

RESULTS

Phenotypic evolution patterns in muroid lineages that underwent a biogeographical transition

Most biogeographical radiations showed no significant increase in Brownian motion rates using the CRT for any of the five ecomorphological traits (Table 2; see also Supporting information, Table S4). Seven of the 30 trait/radiation combinations show significant decreases relative to the background. Only four of these combinations showed the predicted increase: relative tail length and elevation in South America (both a doubling of rate) and mass and PC2 of appendage morphology in Sahul (three- to four-fold increases).

None of the DTT analyses had a significant result for the MDI score ($P > 0.05$) in both the univariate (Fig. 2) and the multivariate (see Supporting information, Fig. S3) analyses. Nonsignificant, negative MDI scores were associated with the primary colonization of Madagascar and South America for PC2 of appendage morphology, Sahul for PC2 of appendage morphology and elevation, and South-east Asia for relative tail length (Fig. 2). Nonsignificant, negative MDI scores were also associated with the primary colonization of Madagascar and Sahul for the multivariate analyses of appendage morphology (see Supporting information, Fig. S3).

The NHT indicated no significant positive relationship between node age and the absolute standardized ICs following any primary colonization, and therefore none experienced the predicted slowdown in the evolutionary rate through time as expected by the niche-filling hypothesis. A significant negative relationship (indicating a speed-up in the rate of evolution through time) was found between node age and the absolute standardized ICs following the primary colonization of: Africa for relative tail length

Table 2. Model parameters of the censored rate test for primary continental colonizations

	σ^2					
		Two-rate				
	One-rate	Foreground	Background	Δ (F – B)	ΔAICc	Rate shift
Africa						
Mass	0.02345	0.02005	0.02373	−0.00368	−1.77	NS
Appendages 1	0.00375	0.00267	0.00385	−0.00118	−0.84	NS
Appendages 2	0.00213	0.00086	0.00224	−0.00138	5.11	Decrease
Tail length	0.01263	0.01131	0.01274	−0.00143	−1.91	NS
Elevation	0.20158	0.26239	0.19647	0.06592	−1.09	NS
Madagascar						
Mass	0.02346	0.02510	0.02340	0.00170	−2.03	NS
Appendages 1	0.00374	0.00084	0.00384	−0.00300	4.48	Decrease
Appendages 2	0.00213	0.00134	0.00215	−0.00081	−1.22	NS
Tail length	0.01262	0.00371	0.01293	−0.00922	3.21	NS
Elevation	0.20182	0.04972	0.20712	−0.15740	4.52	Decrease
North America						
Mass	0.02350	0.01755	0.02422	−0.00667	−0.69	NS
Appendages 1	0.00372	0.00235	0.00388	−0.00153	0.60	NS
Appendages 2	0.00213	0.00035	0.00233	−0.00198	25.43	Decrease
Tail length	0.01260	0.00888	0.01305	−0.00417	−0.14	NS
Elevation	0.20181	0.16258	0.20655	−0.04397	−1.29	NS
South America						
Mass	0.02345	0.01503	0.02605	−0.01102	5.25	Decrease
Appendages 1	0.00374	0.00441	0.00353	0.00088	−0.81	NS
Appendages 2	0.00212	0.00229	0.00207	0.00023	−1.79	NS
Tail length	0.01266	0.02023	0.01033	0.00990	11.40	Increase
Elevation	0.20160	0.32326	0.16408	0.15918	11.64	Increase
Sahul						
Mass	0.02339	0.06787	0.01876	0.04911	27.45	Increase
Appendages 1	0.00374	0.00142	0.00399	−0.00256	7.09	Decrease
Appendages 2	0.00212	0.00632	0.00168	0.00464	26.20	Increase
Tail length	0.01257	0.01018	0.01282	−0.00264	−1.42	NS
Elevation	0.20185	0.15732	0.20649	−0.04917	−1.18	NS
South-east Asia						
Mass	0.02322	0.02374	0.02317	0.00057	−2.05	NS
Appendages 1	0.00367	0.00336	0.00370	−0.00034	−1.97	NS
Appendages 2	0.00213	0.00076	0.00226	−0.00150	7.33	Decrease
Tail length	0.01253	0.01084	0.01270	−0.00187	−1.75	NS
Elevation	0.20156	0.10761	0.21134	−0.10373	2.77	NS

Significant fit of the two-rate parameter model over the one-rate parameter model is based on Δ corrected Akaike information criterion (AICc) > 4 units.
Full output is provided in the Supporting information (Table S4).
σ^2, evolutionary rate; appendages 1 and 2, principal component (PC)1 and PC2; tail length, relative tail length; F, foreground; B, background. NS, not significant.

and elevation; Madagascar for relative tail length; North America for elevation; South America for body mass, relative tail length, and elevation; and South-east Asia for PC2 of appendage morphology and elevation (Fig. 3).

The model comparison (MC) indicated that the EB model did not fit the data best for any of the ecomorphological traits in all biogeographical radiations (Table 3). Out of the 30 trait/radiation combinations, 14 were best fit by the BM model, and the remainder (16) by the OU model. The BAMM analyses indicated that none of the branches were associated with a speciation–extinction rate slowdown or a trait evolution slowdown in any of the five ecomorphological

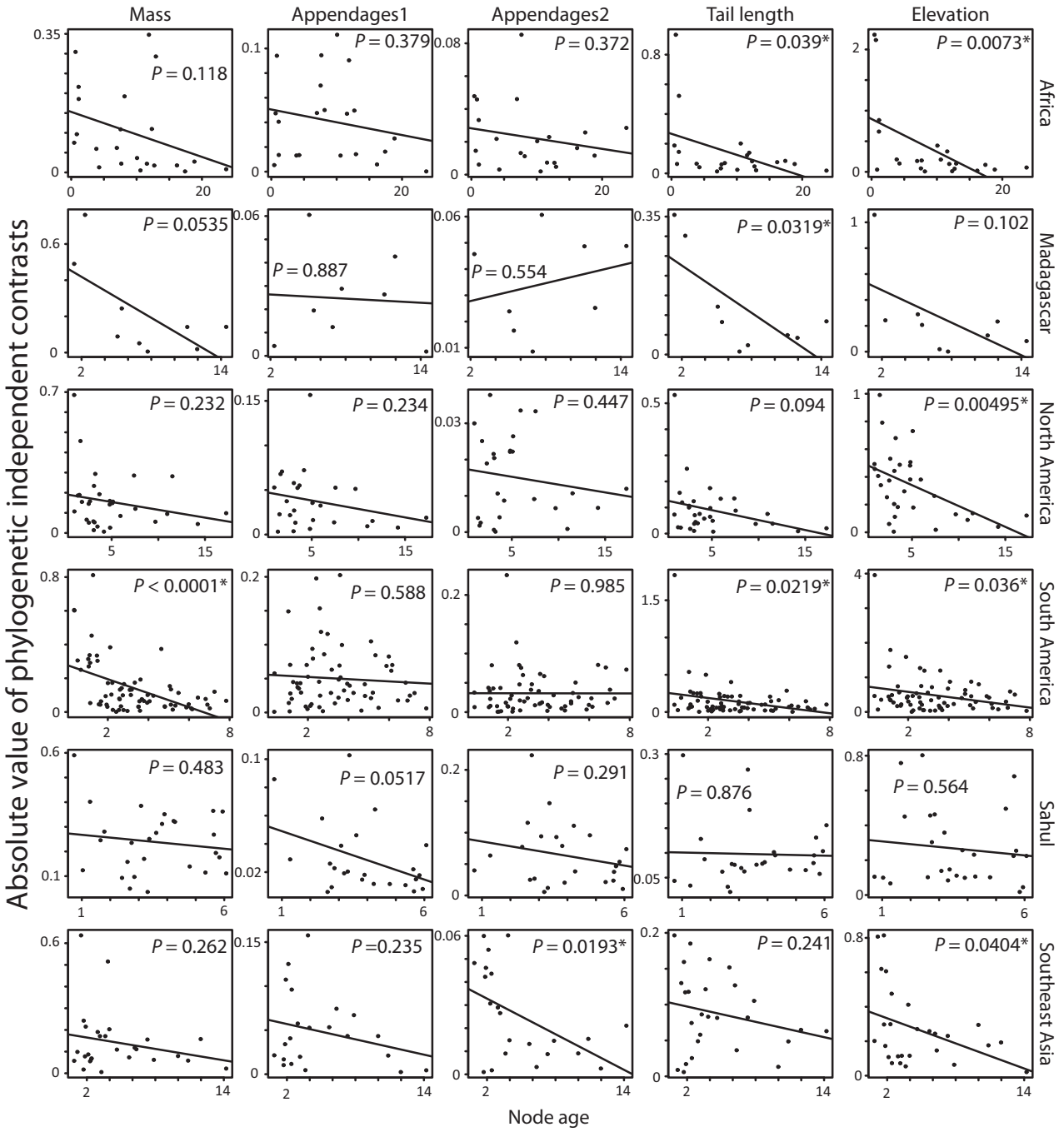

Figure 2. Node height test (NHT) plots for primary continental colonizations. Linear regression lines are indicated. The scales for both the *x*- and *y*-axes differ for each radiation and trait. Appendages 1 and 2, principal component (PC)1 and PC2; tail length, relative tail length. Outliers represent contrasts of shallow nodes and are associated with very short branches, which lead to high rates (e.g. for relative tail length of Muroidea and South America the outlier in the top left corner is the contrast between *Akodon lutescens* and *Akodon boliviensis*).

traits (Fig. 1). The MAP speciation–extinction tree indicates two speed-ups in the rate of diversification, neither of which occurred on the branches leading to the continental colonizations (Fig. 1; SE1-2), although one (SE1) occurred in the branch following the colonization of Africa, just following the Eumuroida. For the trait evolution analyses, the MAP trees indicated: three speed-ups in the rate of evolution of elevation (Fig. 1; EL1–3), one of which occurred on the same branch as the first colonization of South America

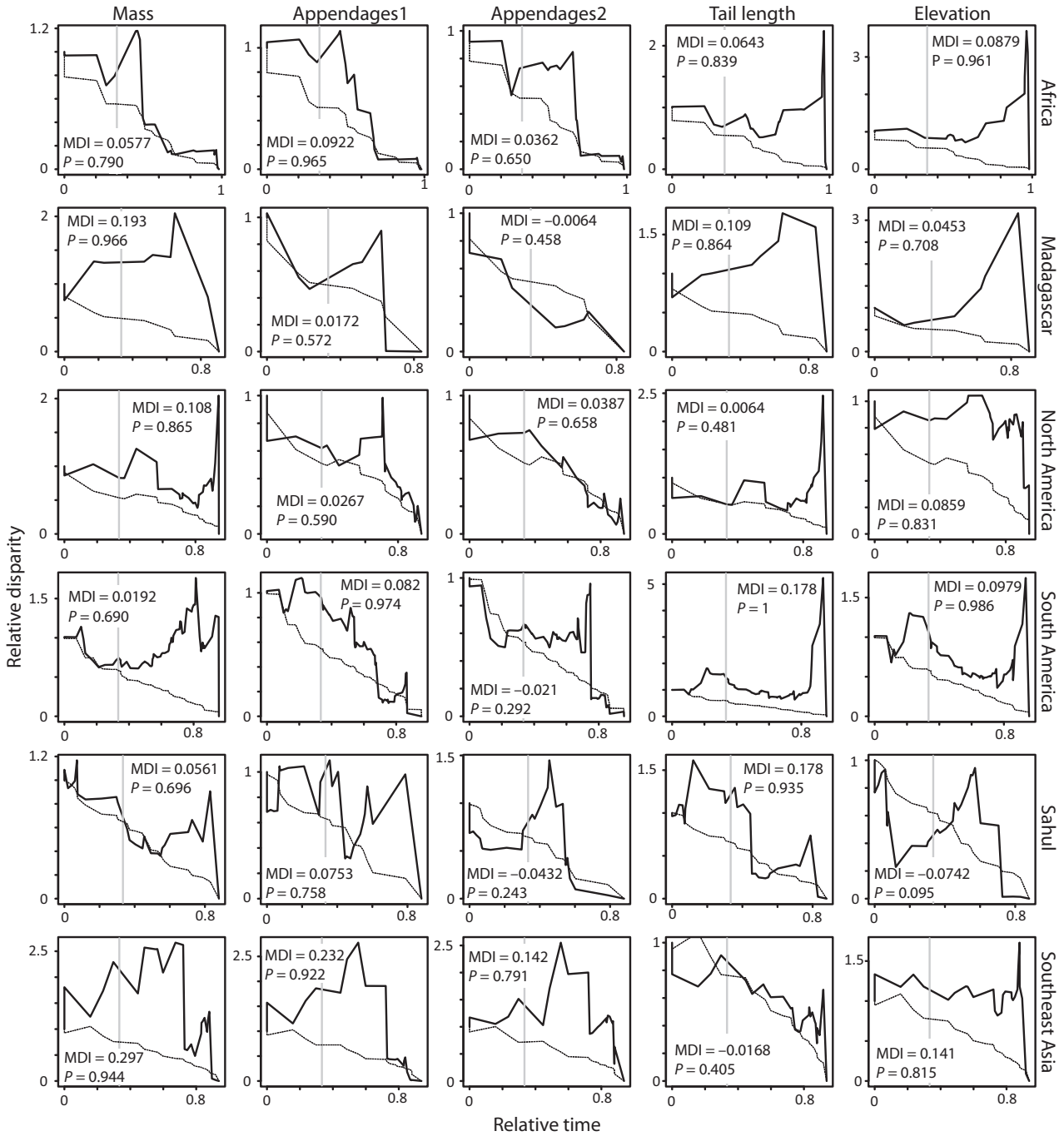

Figure 3. Disparity through time (DTT) plots for primary continental colonizations. Solid lines are the observed disparity and dashed lines are the mean 1000 simulations on the muroid phylogeny under Brownian motion. Morphological disparity index (MDI) scores for the first one-third of the curve, left of the grey line, are indicated, as well as the significance values. Appendages 1 and 2, principal component (PC)1 and PC2; tail length, relative tail length.

(EL2); two speed-ups in the rate of mass evolution (Fig. 1; MA1–2), one of which occurred at the same branch as the colonization of South-east Asia (MA1); one speed-up in the rate of evolution of PC1 of appendage morphology (Fig. 1; PC1.1), not occurring close to branches leading to biogeographical transitions; and three speed-ups in the rate of evolution of PC2 of appendage morphology (Fig. 1; PC2.1–3), none of which occurred on the branches leading to the continental colonizations. The MAP trees for relative tail

Table 3. Relative fit of the Brownian motion (BM), Ornstein–Uhlenbeck (OU), and Early Burst (EB) models to the trait data for primary continental colonizations based on Δ Akaike information criterion (AIC) and AIC weight (AICw)

	ΔAIC			AICw		
	BM	OU	EB	BM	OU	EB
Africa						
Mass	**0.00**	2.00	2.00	**0.58**	0.21	0.21
Appendages 1	1.27	**0.00**	3.27	0.31	**0.58**	0.11
Appendages 2	0.54	**0.00**	2.54	0.37	**0.49**	0.14
Tail length	**0.00**	0.15	2.00	**0.44**	0.40	0.16
Elevation	25.20	**0.00**	27.20	0.00	**1.00**	0.00
Madagascar						
Mass	**0.00**	1.70	2.00	**0.56**	0.24	0.20
Appendages 1	**0.00**	1.31	2.00	**0.53**	0.27	0.20
Appendages 2	**0.00**	1.96	2.00	**0.57**	0.21	0.21
Tail length	**0.00**	2.00	1.06	**0.51**	0.19	0.30
Elevation	3.95	**0.00**	5.95	0.12	**0.84**	0.04
North America						
Mass	**0.00**	2.00	2.00	**0.58**	0.21	0.21
Appendages 1	2.96	**0.00**	4.96	0.17	**0.76**	0.06
Appendages 2	**0.00**	0.37	2.00	**0.45**	0.38	0.17
Tail length	1.64	**0.00**	3.64	0.27	**0.62**	0.10
Elevation	10.12	**0.00**	12.12	0.01	**0.99**	0.00
South America						
Mass	**0.00**	1.19	2.00	**0.52**	0.29	0.19
Appendages 1	0.45	**0.00**	2.45	0.38	**0.38**	0.14
Appendages 2	0.61	**0.00**	2.61	0.37	**0.50**	0.14
Tail length	**0.00**	2.00	2.00	**0.58**	0.21	0.21
Elevation	0.95	**0.00**	2.95	0.34	**0.54**	0.12
Sahul						
Mass	**0.00**	1.70	2.00	**0.56**	0.24	0.20
Appendages 1	3.55	**0.00**	5.55	0.14	**0.81**	0.05
Appendages 2	**0.00**	0.95	2.00	**0.50**	0.31	0.18
Tail length	**0.00**	2.00	1.06	**0.51**	0.19	0.30
Elevation	3.95	**0.00**	5.95	0.12	**0.84**	0.04
South-east Asia						
Mass	**0.00**	1.55	2.00	**0.55**	0.25	0.20
Appendages 1	2.20	**0.00**	4.20	0.23	**0.69**	0.08
Appendages 2	6.46	**0.00**	8.46	0.04	**0.95**	0.01
Tail length	1.92	**0.00**	3.92	0.25	**0.66**	0.09
Elevation	8.71	**0.00**	10.71	0.01	**0.98**	0.00

Bold indicates the best fit model (ΔAIC = 0 and highest AICw). An explanation of trait data abbreviations is provided in Table 2.

length indicated no rate shifts. For BAMM analyses, the only branch with an increased trait evolutionary rate that was close to a branch experiencing an increase in diversification rate was EL3, which occurred on a branch immediately decedent from SE2.

BAMM rates through time plots did not show any major decreases in rates of speciation or trait evolution through time among the radiations descended from the primary colonizations (see Supporting information, Figs S4–S9). There appeared to be a trend towards a speed-up in the rates of elevation evolution through time in Africa (see Supporting information, Fig. S4), PC2 of appendage morphology in North America (see Supporting information, Fig. S6) and Sahul (see Supporting information, Fig. S8), and speciation rate in South-east Asia (see Supporting information, Fig. S9).

Phenotypic evolution patterns in rapidly diversifying muroid clades

Similar to the patterns observed in the muroid lineages that underwent a biogeographical transition, overall, there was little to no support for the two main predictions of EO in rapidly diversifying muroid clades (i.e. clades D1–D9) (Fig. 1) based on CRT, DTT, NHT, MC, and BAMM (Table 4). However, of the nine nodes (D3, D4, D8, and D9) that coincided with increased phylogenetic diversification and are independent of biogeographical transition, four showed some weak patterns consistent with EO. There were increased rates of evolution of several traits relative to the background (see Supporting information, Table S5) and a speed-up in the rate of evolution through time of several traits (see Supporting information, Fig. S10), although several traits had nonsignificant, negative MDI scores (see Supporting information, Fig. S11). Moreover, out of all the non-biogeographical-transition nodes that coincide with increased phylogenetic diversification, only one (D7) fit the data best for EB for only one trait, PC1 (see Supporting information, Table S6); however, this node only consists of six species, and therefore has low power.

DISCUSSION

Are the two main phenotypic predictions of the geographical ecological opportunity model supported in muroids?

We tested EO using disparity and phenotypic evolution as a complement to phylogenetic diversification patterns because they are likely to be less sensitive to the effects of extinction and sampling (Harmon *et al.*, 2003; Slater *et al.*, 2010; Martin & Wainwright, 2011). We tested EO using the censored rates test, disparity through time plots, model comparison, and the node height test, all of which identify focal clades a priori. We also tested for concordance between the a priori identified biogeographical transitions and evolutionary rate shifts identified a posteriori using BAMM. Muroid rodents are an opti-

Table 4. Summary of results for the tests of ecological opportunities (EO) predictions

	Clade	CRT	DTT	NHT	MC	MAP	Comments
	age Mya	increased/ decreased	significant/ nonsignificant	negative/ positive	BM/ OU/EB	speed-up/ slowdown	
Africa	34.1	0/1	0/0	2/0	2/3/0	0/0	
Madagascar	24.5	0/2	0/1	1/0	4/1/0	0/0	
North America	27.4	0/1	0/0	1/0	2/3/0	0/0	
South America	12.3	2/1	0/1	3/0	2/3/0	1/0	Both CRT and NHT = relative tail length and elevation; MAP = elevation
Sahul	9.4	2/1	0/2	0/0	3/2/0	0/0	
South-east Asia	21.4	0/1	0/1	2/0	1/4/0	1/0	
D1	34.1	0/1	0/0	4/0	0/5/0	0/0	
D2	2.8	0/0	0/2	0/0	2/3/0	0/0	
D3	11.6	2/1	0/0	2/0	3/2/0	0/0	Both CRT and NHT = relative tail length
D4	21.4	2/0	0/0	5/0	0/5/0	0/0	
D5	4.6	0/0	0/2	0/0	5/0/0	0/0	
D6	7.9	0/0	0/3	2/0	3/2/0	0/0	
D7	7.0	0/1	1/3	0/0	4/0/1	0/0	Only six species, low power
D8	35.4	1/1	0/0	4/0	0/5/0	0/0	Both CRT and NHT = elevation
D9	12.3	2/1	0/1	3/0	2/3/0	0/0	Both CRT and NHT = relative tail length and elevation

Under CRT, the numbers represent the number of traits that show a significant increase or decrease. Under DTT, the numbers represent the number of traits that show significant negative MDI scores. Under NHT, the numbers indicate the number of traits that show a significant relationship between node age and the absolute standardized ICs. Under MC, the numbers indicate the number of traits that fit the indicated model the best. Under MAP, the numbers indicate the number of traits that show a rate changing on each stem branch.
CRT, censored rate test; DTT, disparity through time; NHT, nodes height test; MC, model comparison (Table 3); MAP, maximum a posteriori analysis (BAMM); Node D1, Eumuroida excluding Calomyscidae; D2, partial *Rattus s.l.*; D3, South America excluding basal groups; D4, South-east Asia plus emigrant radiations in Sahul; Africa; and Eurasian; D5, a subclade within the vole genus *Microtus*; D6, a subclade within Rattini; D7, a subclade within the deer mouse genus *Peromyscus*; D8, Eumuroida; D9, South America plus emigrants to North America.

mal system for testing EO because of their high speciation rate, ecological abundance, high diversity on multiple continents, and frequency of dispersal among those continents. We found little support from disparity and trait evolution for EO, despite the apparent amenability of muroids to EO, as well as the multiple approaches used. The results were similar to those reported by Schenk *et al.* (2013) for phylogenetic diversity; none of the primary continental colonizations were consistent with the main predictions of EO for trait evolution (subsequent to the colonization of a region, there would be a burst of divergence relative to background rates, followed by a decline in those rates). The one exception to this pattern was that the primary colonization of South America was consistent with the EO model for phylogenetic diversification (Schenk *et al.*, 2013) and we found that, out of the very limited support provided for the phenotypic predictions of EO, it was strongest for South America.

No clade arising from a biogeographical transition showed a significantly negative MDI score (Fig. 2). This indicates that early subclade disparity was not lower than expected under Brownian motion, a result that is inconsistent with the EO model (Harmon *et al.*, 2003). Instead, several biogeographical transitions were associated with positive MDI scores, indicating that the ratio of within-subclade disparity to the total was greater than expected under a model of Brownian motion. No clade was associated with a later decline in the rates of evolution of the examined traits (Fig. 3), indicating that none of the clades that underwent a continental colonization experienced the predicted slowdown in the evolutionary rate through time as expected by the niche-filling hypothesis of EO. Instead, all nine significant NHT regressions (out of 30 total for biogeographical transitions) exhibited increasing rates of evolution (Table 4). Of these, only mass for South America was still significant after Bonferroni correction.

Furthermore, when comparing the fit of two common models of evolution (BM and OU) with the explicit time/diversity dependent model of phenotypic evolution, EB, we found that the EB model did not fit the data best for any of the ecomorphological traits in any of the biogeographical radiations (Tables 3, 4). Therefore, we found no support for the EB model in our data, with the BM and OU models being supported, in equal proportions. However, it is important to note that fitting EB models is a difficult process for the small to moderate sample sizes that we analyzed (10–70 taxa).

Similarly, when using a Bayesian approach to test the predictions of EO, we found no support, and BAMM found that none of the branches were associated with a slowdown in the rate of phylogenetic diversification or trait evolution (Fig. 1). Rather, the MAP diversification analyses detected two speed-ups in the rate of diversification, occurring at branches that are not associated with continental colonizations. However, we found minimal support with the MAP trait evolution analyses, where there was a speed-up in rate of evolution of elevation occurring in the same branch as South America (Fig. 1; EL2) and a speed-up in the rate of evolution of body mass occurring in the same branch as South-east Asia (Fig. 1; MA1).

Perhaps, the strongest support for EO (albeit still weak) was detected in the CRT, where two traits each showed a significant increase in Brownian motion rates coincident with the colonization of South America and Sahul (Tables 2, 4). However, among the chosen methods in the present study, CRT is the least optimal in testing the main predictions of the traditional EO model because it does not directly measure a burst but, instead, higher mean rates (i.e. either as result of a burst or parallel acceleration later). CRT simply assumes a shift in rate occurs in two clades, and therefore averages temporally varying rates over entire clades.

Taking the results of all the analyses into account, the general pattern in muroids does not show an early burst followed by a slowdown. Some limited support was detected for accelerated divergence relatively late in the histories of muroid clades. We note that most traits show a pattern under only one test, and therefore there is little consistency among the patterns observed.

Ecological opportunity pattern in 'virgin' colonizations

Oryzomyalia is the clade descended from the colonization of South America by sigmodontines from North America and was the biogeographical transition with the strongest support for the diversity predictions of EO: early burst of speciation followed by a diversity-dependent slowdown (Schenk *et al.*, 2013). This clade has been suggested as an EO/adaptive radiation, although its timing and ecological context has been debated widely (Simpson, 1950; Hershkovitz, 1966; Patterson & Pascual, 1968; Baskin, 1978; D'Elìa, 2003; Parada *et al.*, 2013; Salazar-Bravo, Pardiñas & D'Elía, 2013; Leite *et al.*, 2014).

At the time muroids entered South America, the most ecologically similar mammalian groups consisted of relatively larger caviomorph rodents and marsupials (the latter lacking gnawing incisors) that were unlikely to compete intensely with the muroids (Hooper, 1949; Simpson, 1950; Patterson & Pascual, 1968; Baskin, 1978). The Andes Mountains arose about the same time as Oryzomylaia diversified and may have played a role in that diversification, similar to the pattern previously detected in arboreal caviomorphs (Upham *et al.*, 2013). Nonetheless, the traits that we examined did not support all the predictions of EO in South America with respect to disparity, although we find some support for a speed-up in the evolutionary rate of elevation and relative tail length based on CRT and NHT, and a speed-up in the diversification of elevation only based on BAMM. The only slowdown detected was based on CRT, in a different trait, mass (Table 4).

Sahul, similar to South America, lacked close mammalian competitors at the time that muroids first colonized, approximately 10 Mya, with the mammal fauna being composed of only bats, monotremes, and generally larger marsupials (Schenk *et al.*, 2013). The Sahulian radiation started in New Guinea, and was followed by one or two colonizations of Australia several million years later (Schenk *et al.*, 2013). The colonization of Madagascar by muroids also occurred in the absence of ecologically similar potential rodent competitors. However, despite all this, we failed to detect strong patterns consistent with EO occurring in these colonizations. Similarly, the rest of the colonizations (South-east Asia, North America, and Africa) were inconsistent with EO, which is perhaps less surprising because these regions did have diverse early myodont incumbent communities by the time of these colonizations (Musser & Carleton, 2005) and competitive exclusion from myocricetodontines could explain the lack of EO (Schenk *et al.*, 2013).

Are the two main phenotypic predictions of the ecological opportunity model supported in rapidly diversifying muroid clades?

Other than primary continental colonizations, EO may be triggered by mass extinctions of competitors, the evolution of key innovations or geographical transitions within biogeographical regions (Simpson,

1953; Schluter, 2000a; Grant & Grant, 2008). However, similar to the continental colonizations, the trait-based predictions of EO were generally unsupported along the branches where Schenk *et al.* (2013) found significant increases in the rate of phylogenetic diversification, identified independent of geography.

Moreover, diversification nodes with weak support (i.e. speed-ups with no subsequent slowdowns in the rates of evolution) were close to or at the primary continental colonizations and therefore are influenced by them (e.g. node D3 occurs one node descendant from the primary colonization of South America, node D4 occurs at the same node as the primary colonization of South-east Asia without the removal of emigrating species, and node D9 occurs at the same node as the South American colonization event). This further confirms the lack of support for the phenotypic predictions of the EO model in rapidly diversifying muroid clades. These results are significant (particularly the lack of a burst in morphological evolution/disparity in rapidly diversifying clades) because they provide preliminary evidence that phylogenetic diversification and phenotypic evolution may be decoupled in muroid rodents. The association between phylogenetic diversification and phenotypic evolution is an important focus in current research and has been examined in multiple taxa with mixed results (e.g. plethodontid salamanders show no correlation: Adams *et al.*, 2009; whereas ray-finned fishes exhibit a correlation: Rabosky *et al.*, 2013). We examine this correlation more directly using detailed cranial characters in B. H. Alhajeri & S. J. Steppan (unpublished data).

Potential explanations for the lack of ecological opportunity patterns in muroid rodents

The stage of diversification that we observe could be affected by the age of the radiation. The various colonizations occurred at different times, ranging from 34.1 Mya (Africa) to 9.4 Mya (Sahul). The differences in the timing of the continental colonization could alter the probability to observe a rate slow-down pattern predicted by the EO model. In relatively old radiations such as Africa (34.1 Mya), North America (27.4 Mya), Madagascar (24.5 Mya), and South-east Asia (21.4 Mya), the signature of early bursts may have been erased by extinction. This possibility was suggested for Madagascar by Schenk *et al.* (2013) who also noted that the small area of the island could have led to muroids reaching carrying capacity early, leaving an even longer period of relative equilibrium (Rabosky and Hurlbert, 2015). By contrast, recent radiations such as South America (12.3 Mya) and Sahul (9.4 Mya) may still be in the diversification phase, and have not reached the slowing-down phase. However, the age of colonization did not appear to account for such patterns in species diversification (Schenk *et al.*, 2013).

It is important to note that our conclusions are only met if the traits that we examined are important proxies of ecology. Because we used simple morphological measurements (in addition to elevation), these measurements may not pick up the ecological complexity, and the muroid clades may be radiating with respect to other unmeasured ecological variables, such as diet (which may, or may not be adequately captured by body mass or appendage morphology). Other traits may more effectively capture adaptive divergence, including skull and tooth morphology and a more detailed analysis of limb morphology.

It is also important to note that, although the first phylogenetic prediction of EO (speciation bursts) are not uncommon, the second phylogenetic prediction of EO (subsequent slowdowns) often fail to be detected (e.g. continental bird radiations; Schweizer, Hertwig & Seehausen, 2014). Other than EO, slowdowns in the rate of differentiation (the second phylogenetic prediction of EO) could be a consequence of other factors, such as the pattern of geographical heterogeneity, protracted speciation, extinction or other unrecognized factors (Moen & Morlon, 2015).

Another potential explanation for our general finding of no support for the phenotypic predictions of the EO model and biogeographical transitions is that these transitions did not provide an ecological opportunity for muroids to diversify and exploit new niches. This hypothesis appears unlikely, except perhaps if new niches become more accessible only after transitions to new biomes (e.g. wet tropical forests or semi-arid savannahs) than after transitions to landmasses that may initially be occupied via the ancestral biome. Also, although these muroid clades are rapidly diversifying, this could be explained by other mechanisms such as 'non-adaptive radiation' (Kozak *et al.*, 2006). More likely, EO may simply be too transient a phenomenon to leave a sufficiently strong signal that subsequent radiations or EOs cannot obscure them. Further analyses are needed to assess these alternatives.

CONCLUSIONS

By testing the trait-based predictions of EO using various methods, we have shown that ecological opportunity is not the inevitable consequence of continental colonizations in muroid rodents. Major biogeographical transitions do not appear to lead to ecological-opportunity mediated adaptive radiations

in muroids. EO and its lingering effects may be too transitory, idiosyncratic, and small scale to be detectable by these methods. Moreover, in many clades, radiation can occur in the absence of pre-existing ecological opportunity, and many clades fail to radiate in the presence of ecological opportunity (Losos, 2010). A previous study conducted at a similar large spatial scale (South American ovenbirds) found an analogous pattern to ours; high diversification rates and low morphological evolution (Derryberry *et al.*, 2011). A pattern of high diversification and low morphological evolution (as observed in muroid rodents) may imply that rates of diversification and morphological evolution are decoupled in some taxa (Kozak *et al.*, 2006; Burbrink *et al.*, 2012)

ACKNOWLEDGEMENTS

The manuscript benefited from constructive comments by John Allen, Michael Alfaro, and eight anonymous reviewers. Financial support for this work was provided by a doctoral dissertation fellowship from Kuwait University to BHA (to the Florida State University) and a grant from the National Science Foundation to SJS (DEB-0841447).

REFERENCES

Adams DC, Berns CM, Kozak KH, Wiens JJ. 2009. Are rates of species diversification correlated with rates of morphological evolution? *Proceedings of the Royal Society of London Series B, Biological Sciences* **276:** 2738.

Akaike H. 1974. A new look at statistical model identification. *IEEE Transactions on Automatic Control* **19:** 716–723.

Alexander RM, Vernon A. 1975. The mechanics of hopping by kangaroos (Macropodidae). *Journal of Zoology* **177:** 265–303.

Alfaro ME, Santini F, Brock C, Alamillo H, Dornburg A, Rabosky DL, Carnevale G, Harmon LJ. 2009. Nine exceptional radiations plus high turnover explain species diversity in jawed vertebrates. *Proceedings of the National Academy of Sciences of the United States of America* **106:** 13410–13414.

Allen JA. 1877. The influence of physical conditions in the genesis of species. *Radical Review* **1:** 108–140.

Altshuler DL, Dudley R. 2006. The physiology and biomechanics of avian flight at high altitude. *Integrative and Comparative Biology* **46:** 62–71.

Arctos. 2011. *Arctos. Collaborative Collection Management Solution*, Available at: http://arctos.database.museum (accessed 23 November 2012).

Baldwin BG, Sanderson MJ. 1998. Age and rate of diversification of the Hawaiian silversword alliance (Compositae). *Proceedings of the National Academy of Sciences of the United States of America* **95:** 9402–9406.

Baskin JA. 1978. *Bensonomys*, *Calomys*, and the origin of the phyllotine group of Neotropical cricetines (Rodentia: Cricetidae). *Journal of Mammalogy* **59:** 125–135.

Berman SL. 1985. Convergent evolution in the hindlimb of bipedal rodents. *Journal of Zoological Systematics and Evolutionary Research* **23:** 59–77.

Brown JH. 1995. *Macroecology*. Chicago, IL: University of Chicago Press.

Burbrink FT, Chen X, Myers EA, Brandley MC, Pyron RA. 2012. Evidence for determinism in species diversification and contingency in phenotypic evolution during adaptive radiation. *Proceedings of the Royal Society of London Series B, Biological Sciences* **279:** 4817–4826.

Burnham KP, Anderson DR. 2002. *Model selection and multimodel inference: a practical information-theoretic approach*. New York, NY: Springer.

Cadena CD. 2007. Testing the role of interspecific competition in the evolutionary origin of elevational zonation: an example with Buarremon brush-finches (Aves, Emberizidae) in the neotropical mountains. *Evolution* **61:** 1120–1136.

Chan KMA, Moore BR. 2002. Whole-tree tethods for tetecting differential diversification rates. *Systematic Biology* **51:** 855–865.

Chan KMA, Moore BR. 2005. SymmeTREE: whole-tree analysis of differential diversification rates. *Bioinformatics* **21:** 1709–1710.

Chevret P, Dobigny G. 2005. Systematics and evolution of the subfamily Gerbillinae (Mammalia, Rodentia, Muridae). *Molecular Phylogenetics and Evolution* **35:** 674–688.

Clabaut C, Bunje PME, Salzburger W, Meyer A, Schwenk K. 2007. Geometric morphometric analyses provide evidence for the adaptive character of the Tanganyikan cichlid fish radiations. *Evolution* **61:** 560–578.

D'Elia G. 2003. Phylogenetics of Sigmodontinae (Rodentia, Muroidea, Cricetidae), with special reference to the akodont group, and with additional comments on historical biogeography. *Cladistics* **19:** 307–323.

Derryberry EP, Claramunt S, Derryberry G, Chesser RT, Cracraft J, Aleixo A, Pérez-Emán J, Remsen JV Jr, Brumfield RT. 2011. Lineage diversification and morphological evolution in a large-scale continental radiation: the Neotropical ovenbirds and woodcreepers (Aves: Furnariidae). *Evolution* **65:** 2973–2986.

Drummond CS, Eastwood RJ, Miotto STS, Hughes CE. 2012. Multiple continental radiations and correlates of diversification in *Lupinus* (Leguminosae): testing for key innovation with incomplete taxon sampling. *Systematic Biology* **61:** 443–460.

Endler JA. 1982. Pleistocene refuges: fact or fancy? In: Prance GT, ed. *Biological diversification in the tropics*. New York, NY: Columbia University Press, 641–657.

Fabre PH, Hautier L, Dimitrov D, Douzery E. 2012. A glimpse on the pattern of rodent diversification: a phylogenetic approach. *BMC Evolutionary Biology* **12:** 1–19.

Felsenstein J. 1985. Phylogenies and the comparative method. *American Naturalist* **125:** 1–15.

Flynn LJ, Jacobs LL, Lindsay EH. 1985. Problems in muroid phylogeny: relationship to other rodents and origin

of major groups. In: Luckett WP, Hartenberger JL, eds. *Evolutionary relationships among rodents, a multidisciplinary analysis*. New York, NY: Plenum Press, 589–616.

Fooden J, Albrecht GH. 1999. Tail-length evolution in *Fascicularis*-Group macaques (Cercopithecidae: Macaca). *International Journal of Primatology* **20:** 431–440.

Foote M. 1993. Contributions of individual taxa to overall morphological disparity. *Paleobiology* **19:** 403–419.

Foote M. 1997. The evolution of morphological diversity. *Annual Review of Ecology and Systematics* **28:** 129–152.

Freckleton RP, Harvey PH. 2006. Detecting non-Brownian trait evolution in adaptive radiations. *PLoS Biology* **4:** 2104–2111.

Frédérich B, Sorenson L, Santini F, Slater Graham J, Alfaro ME. 2013. Iterative ecological radiation and convergence during the evolutionary history of damselfishes (Pomacentridae). *American Naturalist* **181:** 94–113.

Futuyma DJ. 1986. *Evolutionary biology, 2nd edn*. Sunderland, MA: Sinauer Associates.

Garland T Jr. 1992. Rate tests for phenotypic evolution using phylogenetically independent contrasts. *American Naturalist* **140:** 509–519.

Google. 2010**.** Google Earth, Version 6.0. Available at: https://earth.google.co.uk.

Grant PR, Grant BR. 2008. *How and why species multiply? The radiation of Darwin's finches*. Princeton, NJ: Princeton University Press.

Hall JPW. 2005. Montane speciation patterns in *Ithomiola* butterflies (Lepidoptera: Riodinidae): are they consistently moving up in the world? *Proceedings of the Royal Society of London Series B, Biological Sciences* **272:** 2457–2466.

Harmon LJ, Schulte JA, Larson A, Losos JB. 2003. Tempo and mode of evolutionary Radiation in iguanian lizards. *Science* **301:** 961–964.

Harmon LJ, Weir JT, Brock CD, Glor RE, Challenger W. 2008a. GEIGER: investigating evolutionary radiations. *Bioinformatics* **24:** 129–131.

Harmon LJ, Melville J, Larson A, Losos JB. 2008b. The role of geography and ecological opportunity in the diversification of day geckos (*Phelsuma*). *Systematic Biology* **57:** 562–573.

Harmon LJ, Losos JB, Jonathan Davies T, Gillespie RG, Gittleman JL, Bryan Jennings W, Kozak KH, McPeek MA, Moreno-Roark F, Near TJ, Purvis A, Ricklefs RE, Schluter D, Schulte JA, Seehausen O, Sidlauskas BL, Torres-Carvajal O, Weir JT, Mooers AØ 2010. Early bursts of body size and shape evolution are rare in comparative data. *Evolution* **64:** 2385–2396.

Hershkovitz P. 1966. Mice, land bridges and Latin American faunal interchange. In: Wenzel RL, Tipton VJ, eds. *Ectoparasites of Panama*. Chicago, IL: Field Museum of Natural History, 725–751.

Hooper ET. 1949. Faunal relationships of recent North American rodents. *Miscellaneous Publications, Museum of Zoology, University of Michigan* **72:** 1–28.

Hurvich CM, Tsai CL. 1989. Regression and time series model selection in small samples. *Biometrika* **76:** 297–307.

Jansa SA, Weksler M. 2004. Phylogeny of muroid rodents: relationships within and among major lineages as determined by IRBP gene sequences. *Molecular Phylogenetics and Evolution* **31:** 256–276.

Jungers WL, Falsetti AB, Wall CE. 1995. Shape, relative size, and size-adjustments in morphometrics. *American Journal of Physical Anthropology* **38:** 137–161.

Kozak KH, Larson A, Bonett RM, Harmon LJ, Schwenk K. 2005. Phylogenetic analysis of ecomorphological divergence, community structure, and diversification rates in dusky salamanders (Plethodontida: *Desmognathus*). *Evolution* **59:** 2000–2016.

Kozak KH, Weisrock DW, Larson A. 2006. Rapid lineage accumulation in a non-adaptive radiation: phylogenetic analysis of diversification rates in eastern North American woodland salamanders (Plethodontidae: *Plethodon*). *Proceedings of the Royal Society of London Series B, Biological Sciences* **273:** 539–546.

LaBarbera M. 1989. Analyzing body size as a factor in ecology and evolution. *Annual Review of Ecology and Systematics* **20:** 97–117.

Lecompte E, Aplin K, Denys C, Catzeflis F, Chades M, Chevret P. 2008. Phylogeny and biogeography of African Murinae based on mitochondrial and nuclear gene sequences, with a new tribal classification of the subfamily. *BMC Evolutionary Biology* **8:** 199.

Leite RN, Kolokotronis SO, Almeida FC, Werneck FP, Rogers DS, Weksler M. 2014. In the wake of invasion: tracing the historical biogeography of the South American cricetid radiation (Rodentia, Sigmodontinae). *PLoS ONE* **9:** e100687.

Lemen C. 1980. Relationship between relative brain size and climbing ability in *Peromyscus*. *Journal of Mammalogy* **61:** 360–364.

Losos JB. 2010. Adaptive radiation, ecological opportunity, and evolutionary determinism. *American Naturalist* **175:** 623–639.

Lovette IJ, Bermingham E. 1999. Explosive speciation in the New World *Dendroica* warblers. *Proceedings of the Royal Society of London Series B, Biological Sciences* **266:** 1629–1636.

Lovette IJ, Bermingham E, Ricklefs RE. 2002. Clade-specific morphological diversification and adaptive radiation in Hawaiian songbirds. *Proceedings of the Royal Society of London Series B, Biological Sciences* **269:** 37–42.

Plummer M, Best N, Cowles K, Vines K. 2010. Coda: output analysis and diagnostics for MCMC. R Package, Version 0.16. Available at: http://cran.rproject.org/web/packages/coda/

Mahler DL, Revell LJ, Glor RE, Losos JB. 2010. Ecological Opportunity and the Rate of Morphological Evolution in the Diversification of Greater Antillean Anoles. *Evolution international journal of organic evolution* **64:** 1–15.

Mahler DL, Ingram T, Revell LJ, Losos JB. 2013. Exceptional convergence on the macroevolutionary landscape in island lizard radiations. *Science* **341:** 292–295.

Mares MA. 2009. *A desert calling: life in a forbidding landscape*. Cambridge, MA: Harvard University Press.

Martin CH, Wainwright PC. 2011. Trophic novelty is linked to exceptional rates of morphological diversification

in two adaptive radiations of *Cyprinodon* pupfish. *Evolution* **65:** 2197–2212.

McCormack JE, Smith TB. 2008. Niche expansion leads to small-scale adaptive divergence along an elevation gradient in a medium-sized passerine bird. *Proceedings of the Royal Society of London Series B, Biological Sciences* **275:** 2155–2164.

McCoy M, Bolker B, Osenberg C, Miner B, Vonesh J. 2006. Size correction: comparing morphological traits among populations and environments. *Oecologia* **148:** 547–554.

McKenna DD, Farrell BD. 2006. Tropical forests are both evolutionary cradles and museums of leaf beetle diversity. *Proceedings of the National Academy of Sciences of the United States of America* **103:** 10947–10951.

McPeek MA. 1995. Testing hypotheses about evolutionary change on single branches of a phylogeny using evolutionary contrasts. *American Naturalist* **45:** 686–703.

McPeek MA. 2008. The ecological dynamics of clade diversification and community assembly. *American Naturalist* **172:** E270–E284.

Moen D, Morlon H. 2015. Why does diversification slow down? *Trends in Ecology & Evolution* **29:** 190–197.

Musser GG, Carleton MD. 2005. Superfamily Muroidea. In: Wilson DE, Reeder DM, eds. *Mammal species of the world, 3rd edn*. Baltimore, MD: The Johns Hopkins University Press, 894–1531.

Navas CA. 2002. Herpetological diversity along Andean elevational gradients: links with physiological ecology and evolutionary physiology. *Comparative Biochemistry and Physiology Part A: Molecular & Integrative Physiology* **133:** 469–485.

Nosil P, Reimchen TE. 2005. Ecological opportunity and levels of morphological variance within freshwater stickleback populations. *Biological Journal of the Linnean Society* **86:** 297–308.

Nowak RM. 1999. *Walker's mammals of the world*. Baltimore, MD: Johns Hopkin University Press.

O'Meara BC, Ané C, Sanderson MJ, Wainwright PC. 2006. Testing for different rates of continuous trait evolution using likelihood. *Evolution* **60:** 922–933.

Parada A, Pardiñas UFJ, Salazar-Bravo J, D'Elía G, Palma RE. 2013. Dating an impressive Neotropical radiation: molecular time estimates for the Sigmodontinae (Rodentia) provide insights into its historical biogeography. *Molecular Phylogenetics and Evolution* **66:** 960–968.

Paradis E, Claude J, Strimmer K. 2004. APE: analyses of phylogenetics and evolution in R language. *Bioinformatics* **20:** 289–290.

Parent CE, Crespi BJ. 2009. Ecological opportunity in adaptive radiation of Galápagos endemic land snails. *American Naturalist* **174:** 898–905.

Patterson B, Pascual R. 1968. Evolution of mammals on southern continents. V. The fossil mammal fauna of South America. *The Quarterly Review of Biology* **43:** 409–451.

Phillimore AB, Price TD. 2008. Density-dependent cladogenesis in birds. *PLoS Biology* **6:** e71.

Polly PD, Lawing AM, Fabre AC, Goswami A. 2013. Phylogenetic principal components analysis and geometric morphometrics. *Hystrix – Italian Journal of Mammalogy* **24:** 33–41.

Porter WP, Sabo JL, Tracy CR, Reichman OJ, Ramankutty N. 2002. Physiology on a landscape scale: plant–animal interactions. *Integrative and Comparative Biology* **42:** 431–453.

Price TD, Hooper DM, Buchanan CD, Johansson US, Tietze DT, Alström P, Olsson U, Ghosh-Harihar M, Ishtiaq F, Gupta SK, Martens J, Harr B, Singh P, Mohan D 2014. Niche filling slows the diversification of Himalayan songbirds. *Nature* **509:** 222–225.

Purvis A, Nee S, Harvey PH. 1995. Macroevolutionary inferences from primate phylogeny. *Proceedings of the Royal Society of London Series B, Biological Sciences* **260:** 329–333.

Quental TB, Marshall CR. 2009. Extinction during evolutionary radiations: reconciling the fossil record with molecular phylogenies. *Evolution* **63:** 3158–3167.

R Development Core Team. 2012. *R: a language and environment for statistical computing*. Available at: http://cran.r-project.org

Rabosky DL. 2014. Automatic detection of key innovations, rate shifts, and diversity-dependence on phylogenetic trees. *PLoS ONE* **9:** e89543.

Rabosky DL, Lovette IJ. 2008. Density-dependent diversification in North American wood warblers. *Proceedings of the Royal Society of London Series B, Biological Sciences* **275:** 2363–2371.

Rabosky DL, Santini F, Eastman J, Smith SA, Sidlauskas B, Chang J, Alfaro ME. 2013. Rates of speciation and morphological evolution are correlated across the largest vertebrate radiation. *Nature Communications* **4:** 1958.

Rabosky DL, Grundler M, Anderson C, Title P, Shi JJ, Brown JW, Huang H, Larson JG. 2014. BAMMtools: an R package for the analysis of evolutionary dynamics on phylogenetic trees. *Methods in Ecology and Evolution* **5:** 701–707.

Rabosky DL, Hurlbert AH. 2015. Species Richness at Continental Scales Is Dominated by Ecological Limits. *The American Naturalist* **185:** 572–583.

Revell LJ. 2009. Size-correction and principal components for interspecific comparative studies. *Evolution: International Journal of Organic Evolution* **63:** 3258–3268.

Rowe KC, Aplin KP, Baverstock PR, Moritz C. 2011. Recent and rapid speciation with limited morphological disparity in the genus Rattus. *Systematic biology* **60:** 188–203.

Rüber L, Zardoya R, Ortí G. 2005. Rapid cladogenesis in marine fishes revisited. *Evolution* **59:** 1119–1127.

Salazar-Bravo J, Pardiñas UFJ, D'Elía G. 2013. A phylogenetic appraisal of Sigmodontinae (Rodentia, Cricetidae) with emphasis on phyllotine genera: systematics and biogeography. *Zoologica Scripta* **42:** 250–261.

Schenk JJ, Rowe KC, Steppan SJ. 2013. Ecological opportunity and incumbency in the diversification of repeated continental colonizations by muroid rodents. *Systematic Biology* **62:** 837–864.

Schluter D. 2000a. *The ecology of adaptive radiation*. Oxford: Oxford University Press.

Schluter D. 2000b. Ecological character displacement in adaptive radiation. *American Naturalist* **156:** S4–S16.

Schweizer M, Hertwig ST, Seehausen O. 2014. Diversity versus disparity and the role of ecological opportunity in a continental bird radiation. *Journal of Biogeography* **41:** 1301–1312.

Simpson GG. 1950. History of the fauna of Latin America. *American Scientist* **38:** 361–389.

Simpson GG. 1953. *The major features of evolution*. New York, NY: Columbia University Press.

Slater GJ, Price SA, Santini F, Alfaro ME. 2010. Diversity versus disparity and the radiation of modern cetaceans. *Proceedings of the Royal Society Series B, Biological Sciences* **277:** 3097–3104.

Steppan S, Adkins R, Anderson J. 2004. Phylogeny and divergence-date estimates of rapid radiations in muroid rodents based on multiple nuclear genes. *Systematic Biology* **53:** 533–553.

Tran LAP. 2014. The role of ecological opportunity in shaping disparate diversification trajectories in a bicontinental primate radiation. *Proceedings of the Royal Society of London Series B, Biological Sciences* **281:** 20131979.

Upham NS, Ojala-Barbour R, Brito MJ, Velazco PM, Patterson BD. 2013. Transitions between Andean and Amazonian centers of endemism in the radiation of some arboreal rodents. *BMC Evolutionary Biology* **13:** 191.

Uyeda JC, Caetano DS, Pennell MW. 2015. Comparative analysis of principal components can be misleading. *Systematic Biology* 1–13.

Walker TD, Valentine JW. 1984. Equilibrium Models of Evolutionary Species Diversity and the Number of Empty Niches. *The American Naturalist* **124:** 887–899.

Yoder JB, Clancey E, Des Roches S, Eastman JM, Gentry L, Godsoe W, Hagey TJ, Jochimsen D, Oswald BP, Robertson J, Sarver BA, Schenk J, Spear SF, Harmon LJ 2010. Ecological opportunity and the origin of adaptive radiations. *Journal of Evolutionary Biology* **23:** 1581–1596.

SUPPORTING INFORMATION

Additional Supporting Information may be found in the online version of this article at the publisher's website:

Figure S1. Biogeographical regions used by Schenk *et al.* (2013) in ancestral-state estimations of primary continental colonizations. Reproduced with permission from Schenk *et al.* (2013): available at: http://datadryad.org/resource/doi:10.5061/dryad.dc34q [CC-BY].

Figure S2. Node height test (NHT) plots for nodes that correspond with biogeographical transition for principal component (PC)1 of appendage morphology. Linear regression lines are indicated. The scales for both *x*- and *y*-axes differ for each radiation and trait. Outliers represent contrasts of shallow nodes and are associated with very short branches, which lead to high rates. These plots were run on standard (nonphylogenetic) size corrected data as opposed to the rest of the analyses in the present study that were run on phylogenetically size corrected data. Compare plots with the plots of 'Appendages 1' in Fig. 2 (which were run on phylogenetically size corrected data).

Figure S3. Disparity through time (DTT) plots for nodes that correspond with biogeographical transition. These DTT plots are multivariate and the disparity is calculated from a matrix that includes appendage data (log-transformed head–body length, log-transformed tail length, log-transformed hind foot length, and log-transformed ear length). The mean DTT from the simulated dataset is represented by a dashed line (mean 1000 simulations) and the empirical DTT in represented by a solid line. Shaded polygons denote the 95% confidence envelope on the distribution of simulated data. Morphological disparity index (MDI) scores for the first one-third of the curve, left of the blue line, are indicated, as well as the significance values.

Figure S4. Plots of rates of speciation through time and trait evolution through time for the primary colonization of Africa. Shaded polygons denote the 95% confidence envelope on the distribution of rates at any point in time.

Figure S5. Plots of rates of speciation through time and trait evolution through time for the primary colonization of Madagascar. Shaded polygons denote the 95% confidence envelope on the distribution of rates at any point in time.

Figure S6. Plots of rates of speciation through time and trait evolution through time for the primary colonization of North America. Shaded polygons denote the 95% confidence envelope on the distribution of rates at any point in time.

Figure S7. Plots of rates of speciation through time and trait evolution through time for the primary colonization of South America. Shaded polygons denote the 95% confidence envelope on the distribution of rates at any point in time.

Figure S8. Plots of rates of speciation through time and trait evolution through time for the primary colonization of Sahul. Shaded polygons denote the 95% confidence envelope on the distribution of rates at any point in time.

Figure S9. Plots of rates of speciation through time and trait evolution through time for the primary colonization of South-east Asia. Shaded polygons denote the 95% confidence envelope on the distribution of rates at any point in time.

Figure S10. Node height test (NHT) plots for nodes with increased phylogenetic diversification. Linear regression lines are indicated. The scales for both *x*- and *y*-axes differ for each radiation and trait. Appendages 1 and 2, principal component (PC)1 and PC2; tail length, relative tail length. Outliers represent contrasts of shallow nodes and are associated with very short branches, which lead to high rates.

Figure S11. Disparity through time (DTT) plots for nodes with increased phylogenetic diversification. Appendages 1 and 2, principal component (PC)1 and PC2; tail length, relative tail length. Solid lines are observed disparity and dashed lines are the mean 1000 simulations on the muroid phylogeny under Brownian motion. Morphological disparity index (MDI) scores for the first one-third of the curve, left of the grey line, are indicated, as well as the significance values.

Table S1. Ecomorphological data for muroid rodents used in phenotypic evolution analyses. Values are based on means of all the data included in the listed references. Mass (g); HBL, head–body length (mm); TL, tail length (mm); HFL, hindfoot length (mm); EL, ear length (mm); Elev, elevation (m asl). Missing data are indicated by a dash (–).

Table S2. Summary of linear regressions between several methods of size correction for the four traits using in the principal component analysis. *b*, coefficient estimate; R^2_{adj}, adjusted R^2 value; Phyl., phylogenetic size-corrected residuals; Non-Phyl., nonphylogenetic size-corrected residuals.

Table S3. Sampling frequencies for each clade used in the BAMM speciation–extinction analysis. The total species number is based on literature sources listed in the main text.

Table S4. Full model parameters of the censored rate test for primary continental colonizations. Significant fit of the two-rate parameter model over the one-rate parameter model is based on a Δ corrected Akaike information criterion (AICc) > 4 units. σ^2, evolutionary rate; Anc, ML ancestral state value; −lnL, negative log likelihood; Appendages 1 and 2, principal component (PC)1 and PC2; tail length, relative tail length.

Table S5. Full model parameters of the censored rate test for nodes with increased phylogenetic diversification. For more information, see Supporting information (Table S2).

Table S6. Relative fit of the Brownian motion (BM), Ornstein–Uhlenbeck (OU), and Early Burst (EB) models to the trait data for nodes with exceptional diversification based on Akaike information criterion (AIC), Δ corrected AIC (AICc), and AIC weight (AICw). The use of bold indicates the best fit model (lowest AIC, ΔAIC = 0, and highest AICw). An explanation of the trait data abbreviations is provided in the Supporting information (Table S2).